\$ SUPER

Contents lists available at ScienceDirect

International Journal of Pharmaceutics

journal homepage: www.elsevier.com/locate/ijpharm



Reverse-dialysis can be misleading for drug release studies in emulsions as demonstrated by NMR dilution experiments



Zhaoyuan Gong ^{a,1}, Mohammad Hossein Tootoonchi ^{b,1}, Christopher A. Fraker ^{b,2}, Jamie D. Walls ^{a,*}

- a Department of Chemistry, University of Miami, Coral Gables FL 33146, United States
- b Diabetes Research Institute, University of Miami Miller School of Medicine, Miami FL 33136, United States

ARTICLE INFO

Keywords:
Reverse-dialysis
Nuclear magnetic resonance
Release kinetics
Isoflurane
Emulsions
Chemical exchange

ABSTRACT

Emulsions are an important class of carriers for the delivery of hydrophobic drugs. While knowledge of drug release kinetics is critical to optimizing drug carrying emulsions, there remain many open questions about the validity of standard characterization methods such as the commonly used reverse-dialysis. In this paper, the kinetic parameters of isoflurane release in perfluorotributylamine emulsions determined from both reverse-dialysis and nuclear magnetic resonance (NMR) dilution experiments are compared. The NMR-determined kinetic parameters of isoflurane release were found to be approximately *seven orders of magnitude* larger than those determined from conventional reverse-dialysis and were also shown to be consistent with prior *in vivo* observations of the anesthetization of rats.

1. Introduction

Emulsions are a subject of interest as drug carriers with many clinically approved formulations already available in the marketplace (Zhong et al., 2018; Salva et al., 2017). A necessary step in the design of drug/emulsion formulations is the characterization of the drug release kinetics. Dialysis, filtration, and centrifugation are among the most common techniques that have been used to perform kinetic studies on nanoparticulate drug delivery systems (Shen and Burgess, 2013; D'Souza and DeLuca, 2006; Solomon et al., 2017). Alternative methods based upon flow cytometry have also been used (D'Addio et al., 2016; Petersen et al., 2010). However, questions about the validity of such methodologies to accurately capture release kinetics have been raised (Levy and Benita, 1990; Bernkop-Schnurch and Jalil, 2018; Washington, 1990; Washington, 1989; Zambito et al., 2012). For example, a study by Washington et al. demonstrated using a stop flow technique that drug release kinetics can be occurring on timescales much faster than the detection limits of conventional approaches (Salmela and Washington,

One of the most common methods for characterizing drug release kinetics is reverse-dialysis (Levy and Benita, 1990), whereby a Albeit to a lesser extent than reverse-dialysis, nuclear magnetic resonance (NMR) has also been employed to characterize the real-time slow release of drugs using quantitative or q-NMR techniques (Agrahari et al., 2017). Unlike reverse-dialysis and q-NMR, however, the majority of NMR drug release studies do not monitor drug release in real-time but are instead performed under equilibrium conditions (Hey

E-mail address: jwalls@miami.edu (J.D. Walls).

nanocarrier's drug release kinetics are determined by monitoring the drug concentration inside a dialysis sac that is impermeable to the nanocarrier. An important assumption in using reverse-dialysis to characterize drug release kinetics is that the drug can freely enter the dialysis sac on a timescale that is much faster than the drug release from the nanocarriers. However, it has been pointed out that this assumption can be violated if drug release rates are much faster than the timescale of drug diffusing into the dialysis sac and/or if the drug is poorly water-soluble (Modi and Anderson, 2013; Abouelmagd et al., 2015). In such cases, modest discrepancies between drug release times derived from reverse-dialysis and alternative measurement methodologies have been previously noted (Forrest et al., 2018; Moreno-Bautista and Tam, 2011; Xie et al., 2015). In spite of these potential pitfalls, reverse-dialysis continues to be one of the most common methods for characterizing nanocarrier drug release kinetics.

^{*} Corresponding author.

¹ Contributed equally to this work.

² Co-senior author.

and Al-Sagheer, 1994). In such cases, information about the drug release kinetics can still be determined by exploiting differences in a drug's spectral and/or physical parameters between the aqueous or organic phases. For example, diffusion-based NMR methods (Johns and Hollingsworth, 2007) have been used to provide drug release kinetics of propofol in emulsions due to differences in propofol's self-diffusion coefficient in aqueous and organic environments (Momot et al., 2003; Momot and Kuchel, 2003). Monitoring NMR chemical shift changes using titration/dilution experiments has also been used to determine K_D , which is a drug's partition coefficient between aqueous and hydrophobic phases within an emulsion (Kreilgaard and Pedersen, 2000; Omran et al., 2002). As was the case with reverse-dialysis, it is challenging to extract drug release kinetic parameters using the above NMR techniques in situations where the drugs are poorly water-soluble and/or where the drug release kinetics are faster than the differences in spectral parameters.

Recently, the authors demonstrated that kinetic exchange rate constants in emulsions could be determined from a series of NMR dilution experiments by fitting both chemical shifts and line widths (Gong et al., 2021). In this work, both reverse-dialysis and NMR-dilution experiments were used to measure the *in vitro* release of the poorly water-soluble drug, isoflurane, from an injectable anesthetic composed of an emulsified solution of isoflurane in perfluorotributylamine (FC43) (Ashrafi et al., 2018; Pretto et al., 2016; Pretto et al., 2018). As will be demonstrated, the NMR-determined isoflurane release times were found to be approximately *seven orders of magnitude* faster than those determined from conventional reverse-dialysis measurements.

2. Materials and methods

2.1. Emulsion preparation and characterization

Temperature controlled high pressure (15,000 PSI) homogenization using a ShearJet™ HL60 from Dyhydromatics (Maynard, MA, USA) was used to emulsify a 1:1 v/v isoflurane/FC43 solution in a 20% v/v ratio with a saline solution [normal saline (sodium chloride(aq) 0.9% w/v) containing 2% w/v of the surfactants, pluronic F68 and F127, in a 1:1 ratio to stabilize the emulsion droplets (see Ref. (Fraker et al., 2012) for more details)]. All preconcentrates were prepared between 8 and 12 $^{\circ}$ C. The hydrodynamic diameters for two different emulsion formulations, denoted as E1 and E2, were characterized by dynamic light scattering (DLS) experiments performed on a Malvern Zetasizer Nano ZS with a noninvasive back scatter configuration at 13 + 173 degrees. The diluent used was normal saline, which has a viscosity of 1 cP at T=298 K. The algorithms available through the Zetasizer software used a general purpose, non-negative least squares method by Lawson and Hanson (1974) to fit the particle size distribution. The average hydrodynamic diameters are given in Table 1. As shown in Supporting Information, dilutions greater than 40× were needed in order to reduce the effects of particle-particle interactions and multiple scattering on the apparent hydrodynamic

The isoflurane content of the emulsions was determined using high performance liquid chromatography (HPLC). First, standard samples were prepared by mixing 100 μ L, 50 μ L, and 25 μ L of isoflurane with 900 μ L, 950 μ L, and 975 μ L of methanol in 1.25 mL shell vials (Fisher

Table 1Characterization of the undiluted emulsions used in this study.

Emulsion	[Iso] _{tot} (mM) ^a	$d_{\rm Emul} ({\rm nm})^{\rm b}$	Specific area $\left(\frac{cm^2}{mL}\right)^c$
E1	750 ± 20	191.8 ± 1.2	6.00×10^4
E2	787 ± 9	161.9 ± 1.0	7.30×10^4

^a Total isoflurane concentration determined by HPLC.

Scientific). These standards were then diluted $10\times$ twice to produce a total of nine standards corresponding to 10%, 5%, 2.5%, 1%, 0.5%, 0.25%, 0.1%, 0.05%, and 0.025% isoflurane. Pure methanol was used as the 0% standard, and fresh standards were prepared for every measurement. For the HPLC measurements of the emulsions, 100 μL of emulsion was mixed with 900 μL of methanol in a 1.25 mL shell vial, capped and vortexed for 1 min to break up the emulsion. The resulting solution was transparent with an immiscible layer of FC43 at the bottom. Both methanol and FC43 are maximally miscible with isoflurane, which was the rationale for using methanol in the emulsion fracture.

All HPLC measurements were acquired on a Hitachi Lachrom Elite instrument. The quantitative measurements were performed at 30 °C on an Ascentis® C18 (15 cm \times 4.6 mm i.d., 5 µm) with photodiode array detection at 203 nm. The mobile phase was water:acetonitrile, 40:60 (v/v). Elution was done at 0.6 mL/min for 10 min. A 20 µL injection was used for both standards and samples, and a 100 µL injection was used for the dialysis samples described below. Each sample was run 3 times, and the column was washed between each run by running 10 µL of pure methanol. Standard samples were run only once. The peak at 6 to 7 min corresponded to isoflurane and was integrated using the commercial software provided with the instrument.

2.2. Stability of the emulsions under dilution

Samples of both E1 and E2 emulsions were diluted by adding 17.17 μL , 6.83 μL and 3.41 μL of the emulsion to 1700 μL of a diluent to produce $100\times$, $250\times$ and $500\times$ dilutions, respectively. Two diluents were used: saline and isoflurane saturated saline (the preparation of which is described in Supporting Information). Each sample was prepared in triplicate. Samples were sealed, mixed by shaking and placed inside a temperature controlled oven at 29 ± 2 °C. One replicate of each sample was removed at 1 h, 2 h, 4 h, 6 h, 24 h, and 96 h time points, and its particle size was measured using DLS. For each configuration, one sample was measured by DLS at t=0 without experiencing elevated temperature as a control.

2.3. Reverse-dialysis measurements

Reverse-dialysis was performed using Thermo Fisher Scientific's Snakeskin™ 10 k MWCO, 22 mm dialysis tubing. The tube was cut into 5 cm pieces and soaked in deionized water for 30 min. It was then folded and clamped on both ends, holding 1.5 mL of saline inside. Each sac along with a magnetic stirrer were placed inside a 100 mL glass media bottle containing 128.5 mL normal saline [each media bottle (Duran®, Schott AG) had an actual available volume of approximately 138 mL when measured up to the bottle's lip]. The bottles were then capped and placed in an oven at 29 \pm 2 $^{\circ}\text{C}.$ For the reverse-dialysis measurements of the emulsions, 1.314 mL of a given emulsion was added to each bottle, resulting in an overall dilution of $100 \times$. The bottles were then sealed and stirred at 60 rpm at 29 ± 2 °C. Eight bottles were prepared as described above with a bottle removed from the oven at times 5 min, 10 min, 20 min, 30 min, 45 min, 60 min, 90 min, and 120 min after addition of the emulsion. Once removed, 1 mL samples were taken from inside and outside of the dialysis sac. The isoflurane content of each sample was measured using HPLC as described above without breaking the emulsion in methanol. The above procedure was repeated n = 3 times for each emulsion.

As a control experiment, bottles were also prepared with 130 mL of isoflurane saturated saline solution ([Iso] $_{\rm aq}=9.7$ mM) that were capped and placed in an oven at 29 ± 2 °C. For the reverse-dialysis measurements, magnetic stirrers and dialysis sacs containing 1.5 mL of saline were added to the seven such bottles, which were then sealed and stirred at 60 rpm. A bottle was removed from the oven at times 5 min, 10 min, 20 min, 30 min, 45 min, 60 min, and 120 min after the addition of the dialysis sacs, whereupon 1 mL samples were again taken from inside and outside of the dialysis sac with the isoflurane content of each sample

 $^{^{\}text{b}}\,$ Determined from DLS at 100× dilution.

 $^{^{}m c}$ Calculated using $d_{
m Emul}$ and the volume fraction of the emulsion droplets.

measured using HPLC. This procedure was repeated n=3 times. Plots of the isoflurane content inside the dialysis sacs relative to the isoflurane content outside the dialysis sacs are given in Fig. 2b.

2.4. NMR dilution measurements

The ¹H NMR spectra were acquired on a 300 MHz Bruker AVANCE NEO spectrometer equipped with an automatic sample changer using the pulse sequence "zgcpgppr" available in the Bruker library. The transmitter was always set to the water resonance, and a 50 Hz presaturation pulse was applied to suppress any residual water signal. The following acquisition parameters were used in all experiments: a repetition time of 30 s, a dwell time of 333 µs (corresponding to a spectral width of 10 ppm), and an acquisition time of 3 s. The number of scans (NS) was varied for different dilution samples to achieve a desired signal-to-noise ratio with NS <512. All ¹H NMR spectra were acquired within 24 h of sample preparation as the DLS results in Fig. 1 indicated that the emulsions were stable over this time period (dilution protocols are given in Supporting Information). The determination of rate constants in emulsions from the NMR dilution spectra has been presented elsewhere (Gong et al., 2021). Briefly, isoflurane chemical shifts and line widths were determined at each dilution by deconvolving the individual isoflurane resonances in the ¹H NMR spectrum. The kinetic rate constants were then determined by simple algebraic calculations using the observed chemical shifts and line widths as inputs.

2.5. NMR diffusion studies

Self diffusion coefficients were measured for isoflurane and FC43 using a stimulated echo with bipolar gradient and longitudinal eddy current delay (LED) sequence [Fig. 4a], implemented by the "ledbpgp2s" pulse program in the Bruker library (Gibbs and Johnson, 1991). All experiments were performed on a 400 MHz Bruker spectrometer with an LED time of $\Delta_{\rm LED}=5$ ms. Both $^{1}{\rm H}$ and $^{19}{\rm F}$ NMR were used to measure the self-diffusion coefficients of isoflurane and FC43, respectively, by fitting the decay of the NMR signals with increasing gradient strength, **g**, to the standard decay curve(Sinnaeve, 2012) given by:

$$\ln\left(\frac{S(\mathbf{g})}{S(0)}\right) = -4D(\sigma\gamma\mathbf{g}\delta)^{2}\left(\Delta + \frac{(2\kappa - 2\lambda - 1)\delta}{2} - \tau\right) \tag{1}$$

where γ is the gyromagnetic ratio for a given nucleus ($^1\text{H or }^{19}\text{F}$), D is the self-diffusion coefficient, δ is the gradient pulse length, τ is the gradient stabilization delay, and Δ is the diffusion time. In Eq. (1), σ,κ , and λ are numerical parameters that are determined by the particular pulsed

gradient pulse shape used in the diffusion sequence in Fig. 4a. For the smoothed rectangular gradient pulses used in this work(Sinnaeve, 2012), $\sigma = \frac{9}{10}$, $\lambda = \frac{1}{2}$, and $\kappa \approx 0.3495$. In the diffusion studies, 16 constant time gradients with varying **g** were used to generate the experimental diffusion decay curve for the FC43 and isoflurane resonances that were fit to Eq. (1). Different NS, δ , and Δ were used to obtain a desired signal to noise ratio along with a full decay curve given by Eq. (1) such that $\left|\frac{S(\mathbf{g})}{S(0)}\right| \left\langle 0.05 \right|$ for the largest **g** used. A dwell time of 250 μ s and a total acquisition time of 1.5 s were used in all diffusion studies.

3. Results and discussion

3.1. Reverse-dialysis

A sketch of a reverse-dialysis setup is shown in Fig. 2a, where the exchange of isoflurane between the aqueous and organic phases (the latter represented by spherical droplets) and the exchange of isoflurane between the external aqueous phase and a dialysis sac that is impermeable to the emulsion droplets are illustrated. The basic kinetic equations can be written as:

$$Iso + Emul \underset{\stackrel{R.D.}{\stackrel{}{\sim}}}{\underset{R.D.}{\rightleftharpoons}} Iso_{Emul}$$
 (2)

$$Iso \underset{\frac{V_{aq}}{V_{dh}}_{db}}{\overset{k_{db}}{\rightleftharpoons}} Iso_{db}$$
 (3)

where Iso, Iso_{Emul}, and Iso_{dh} denote isoflurane in the aqueous phase, in an emulsion droplet, and in a dialysis sac, respectively, and Emul denotes an emulsion droplet. Eqs. (2) and (3) represent a simplified version of measuring drug release rates via reverse-dialysis, where an instantaneous, homogeneous equilibration of the isoflurane concentration in the aqueous phase is assumed (see Ref. (Modi and Anderson, 2013) for more detailed models of reverse-dialysis). With this simplified model, however, if (I) the volume of the dialysis sac ($V_{\rm db}$) is much smaller than the volume of the aqueous phase outside of the dialysis sac (V_{aq}) such that $V_{\rm db} + V_{\rm aq} \approx V_{\rm aq}$ is a reasonable approximation, and (II) the exchange of isolfurane between the aqueous phase and the dialysis sac in Eq. (3) represents a fast equilibrium, i.e., $k_{\text{db}}\gg \kappa_{\text{in}}^{\text{R.D.}}[\text{Emul}] \& k_{\text{out}}^{\text{R.D.}}$, then the concentration of isoflurane within the dialysis sac $\left([\text{Iso}(t)]_{\text{db}} = \frac{n_{\text{Iso},\text{db}}(t)}{V_{\text{db}}}, \right)$ where $n_{\rm Iso,db}(t)$ is the number of moles of isoflurane in the dialysis sac) will reflect the instantaneous concentration of isoflurane within the aqueous phase $\left([\text{Iso}(t)]_{\text{aq}} = \frac{n_{\text{Iso,aq}}(t)}{V_{\text{aq}}}, \text{ where } n_{\text{Iso,aq}}(t) \text{ is the number of moles} \right)$

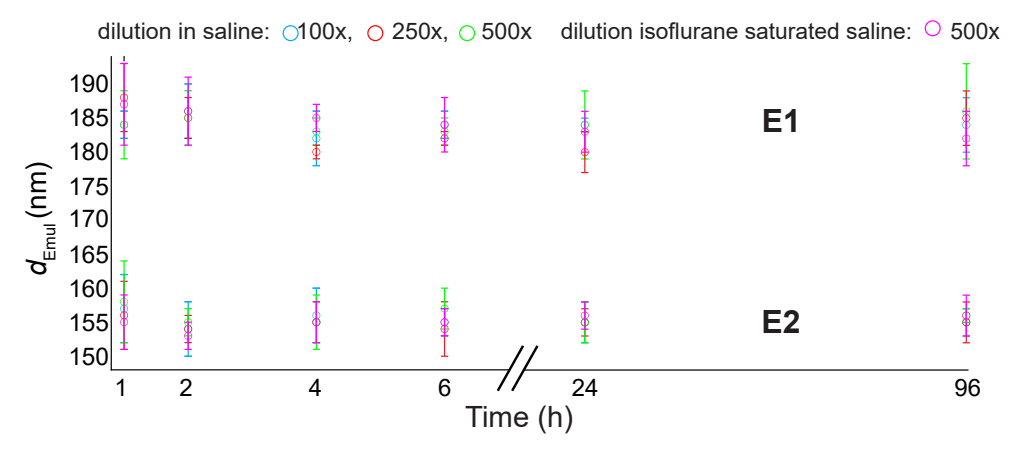


Fig. 1. : Particle size measured by DLS after incubation at 29 ± 2 °C of the E1 (top, $d_{\text{Enull}} = 184 \pm 4$ nm) and E2 (bottom, $d_{\text{Enull}} = 156 \pm 4$ nm) emulsions for different dilutions in normal saline [100× (blue), 250× (red), 500× (green)] and in isoflurane saturated normal saline [500× (magenta)] at times of 1 h, 2 h, 4 h, 6 h, 24 h, and 96 h. These results suggest that the emulsions were stable in excess of 96 h.

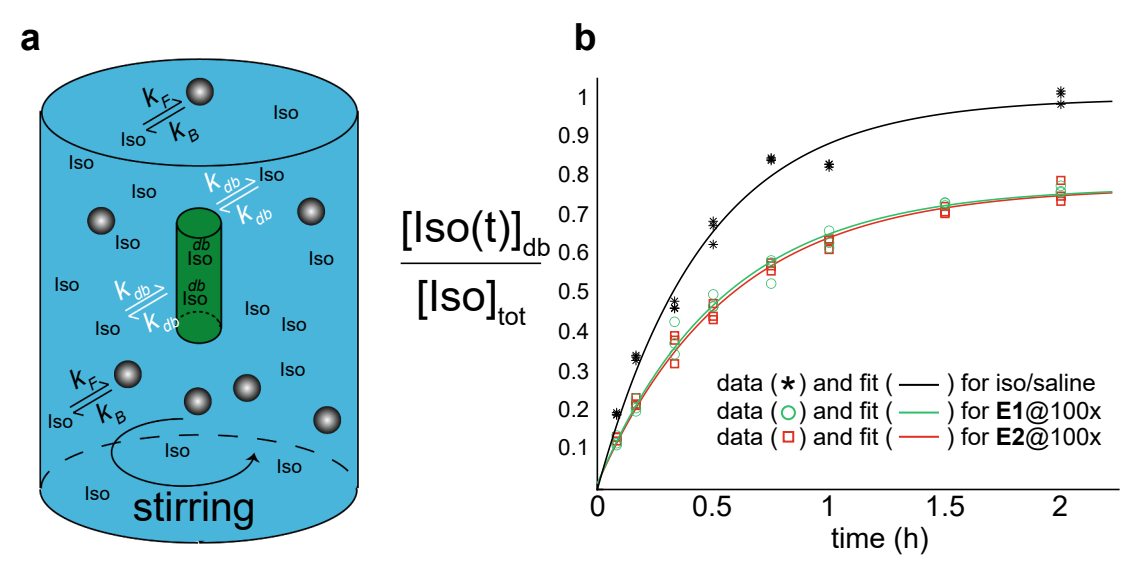


Fig. 2. Reverse-dialysis measurements of isoflurane release. a Schematic for the reverse-dialysis measurements illustrating isoflurane (Iso) release from emulsions (denoted by spheres) under $100 \times$ dilution and transport into a dialysis sac (green cylinder). b Experimental release profile of isoflurane measured by reverse-dialysis. Each measurement was repeated n=3 times [experimental results for (green circles) E1 and (red squares) E2 emulsions and for the (black asterisks) control experiments using an isoflurane saturated saline solution]. Solid curves represent the best fit curves to Eq. (5) for the emulsions and to Eq. (10) for the control experiments.

of isoflurane in the aqueous phase) at all times, i.e., $[\mathrm{Iso}(t)]_{\mathrm{db}} \approx [\mathrm{Iso}(t)]_{\mathrm{aq}}$. With these assumptions, $[\mathrm{Iso}(t)]_{\mathrm{aq}}$ can be determined by solving the following kinetic equations derived under the conditions of mass balance (see Supporting Information for more details):

$$\frac{\mathrm{d}[\mathrm{Iso}(t)]_{\mathrm{aq}}}{\mathrm{d}t} = -\kappa_{\mathrm{in}}^{\mathrm{R.D.}}[\mathrm{Emul}][\mathrm{Iso}(t)]_{\mathrm{aq}} + \frac{V_{\mathrm{FC43}}}{V_{\mathrm{aq}}}k_{\mathrm{out}}^{\mathrm{R.D.}}[\mathrm{Iso}(t)]_{\mathrm{Emul}}$$

$$\frac{\mathrm{d}[\mathrm{Iso}(t)]_{\mathrm{Emul}}}{\mathrm{d}t} = \frac{V_{\mathrm{aq}}}{V_{\mathrm{FC43}}} \kappa_{\mathrm{in}}^{\mathrm{R.D.}} [\mathrm{Emul}] [\mathrm{Iso}(t)]_{\mathrm{aq}} - k_{\mathrm{out}}^{\mathrm{R.D.}} [\mathrm{Iso}(t)]_{\mathrm{Emul}}$$
(4)

where $[\mathrm{Iso}(t)]_{\mathrm{Emul}} = \frac{n_{\mathrm{Iso,org}}(t)}{V_{\mathrm{IC43}}}$ represents the concentration of isoflurane within the emulsion droplets with respect the total FC43 volume, V_{FC43} , and $[\mathrm{Emul}]$ represent the sample molar concentration of emulsion droplets with respect to the total sample volume, V_{tot} . Since the total number of moles of isoflurane is constant, $n_{\mathrm{Iso,tot}} = V_{\mathrm{tot}} [\mathrm{Iso}]_{\mathrm{tot}} \approx V_{\mathrm{aq}} [\mathrm{Iso}(t)]_{\mathrm{aq}} + V_{\mathrm{FC43}} [\mathrm{Iso}(t)]_{\mathrm{Emul}}$ at all times t, Eq. (4) can be solved to give:

$$[\operatorname{Iso}(t)]_{db} \approx [\operatorname{Iso}(t)]_{aq} = [\operatorname{Iso}]_{aq,eq} + ([\operatorname{Iso}(0)]_{aq} - [\operatorname{Iso}]_{aq,eq}) \exp\left(-\frac{t}{\tau_{\text{R.D.}}}\right)$$
 (5)

$$[Iso]_{aq,eq} = k_{out}^{R.D.} \tau_{R.D.} \frac{V_{tot}}{V_{ao}} [Iso]_{tot}$$

$$(6)$$

$$[Iso(t)]_{Emul} = [Iso]_{Emul,eq} + ([Iso(0)]_{Emul} - [Iso]_{Emul,eq}) \exp\left(-\frac{t}{\tau_{R.D.}}\right)$$
(7)

$$[Iso]_{Emul,eq} = \kappa_{in}^{R.D.}[Emul]\tau_{R.D.} \frac{V_{tot}}{V_{FC43}}[Iso]_{tot}$$
(8)

where $\tau_{R,D}$ is the isoflurane release time given by:

$$\tau_{\text{R.D.}} = \frac{1}{\kappa_{\text{in}}^{\text{R.D.}}[\text{Emul}] + k_{\text{out}}^{\text{R.D.}}} \equiv \frac{1}{k_{\text{exch}}^{\text{R.D.}}}$$
(9)

For the control experiments, only the diffusion into and out of the dialysis sac in Eq. (3) are relevant, which gives:

$$[Iso(t)]_{db}^{control} = [Iso]_{tot} \left(1 - \exp\left(-\frac{t}{\tau_{control}} \right) \right)$$
 (10)

where τ_{control} is given by:

$$\tau_{\text{control}} = \frac{V_{\text{db}}}{(V_{\text{aq}} + V_{\text{db}})k_{\text{db}}} = \frac{V_{\text{db}}}{V_{\text{tot}}k_{\text{db}}}$$
(11)

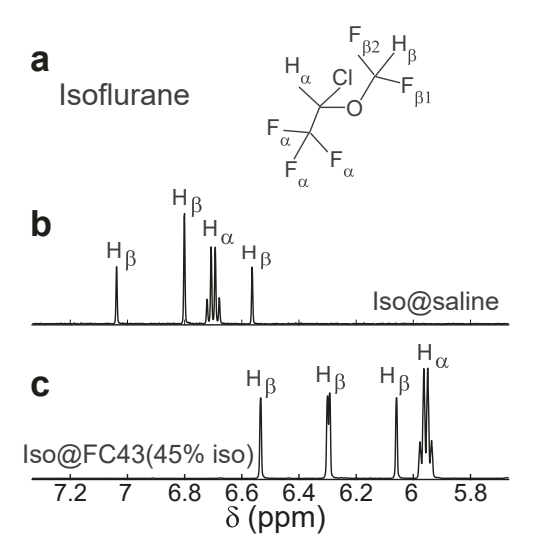
In Fig. 2b, the results from reverse-dialysis measurements are shown for the E1 and E2 emulsions (Table 1) that were initially diluted $100 \times$ in normal saline to simulate the dilution of an induction bolus dose in the bloodstream (Ashrafi et al., 2018). The buildup of isoflurane within the dialysis sacs was fit to Eq. (5) using the "fit" function in MATLAB from which both $\kappa_{\rm in}^{\rm R.D.}$ and $k_{\rm out}^{\rm R.D.}$ were determined. Both the kinetic parameters and release times [Eq. (9)] determined from the reverse-dialysis measurements given in Fig. 2b are listed in Table 2. The steady-state values for $\frac{[Iso(t)]_{db}}{[Iso]_{or}}$ in Fig. 2b were $(77\pm1)\%$ and $(76\pm3)\%$ for the E1 and E2 emulsions, respectively, which were approximately 88 –89% smaller than the predicted value of 87% found using the K_D of isoflurane between FC43 and saline (see Supporting Information for more details). Similarly, a fit of the control data to Eq. (10) is also shown in Fig. 2b [black curve and asterisks] which gave $\tau_{control} = (1740 \pm 60)$ s. Thus the time constant for isoflurane entering a dialysis sac was comparable to the apparent isoflurane release time determined from reverse-dialysis, i. e., $\tau_{control} \sim \tau_{R.D.}$. This suggests that the assumption that isoflurane entering the dialysis sac was much faster than isoflurane release from the emulsion droplets, which was used to derive $[Iso_{db}(t)] \approx [Iso_{ad}(t)]$ in Eq. (4), does not appear to be justified.

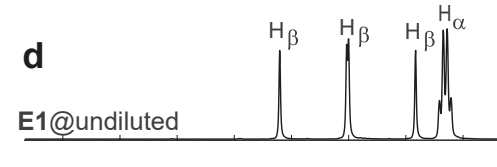
3.2. NMR studies

As shown in Fig. 3a, isoflurane contains two chemically distinct 1 H nuclei, H_{α} and H_{β} . As a result of spin-spin couplings to neighboring 19 F

Table 2 Kinetic parameters for isoflurane in emulsions determined by reverse dialysis experiments at $100\times$ dilution shown in Fig. 2b. The uncertainties represent the standard deviations after averaging over 3 replicates.

Emulsion	$k_{ m out}^{ m R.D.}~(imes 10^{-4}~{ m s}^{-1})$	$\kappa_{\rm in}^{R.D.}$ ($\times~10^4~M^{-1}~{\rm s}^{-1})$	$\tau_{\rm R.D.}$ (s)
E1	3.9 ± 0.1	13 ± 1	1960 ± 90
E2	3.8 ± 0.1	7.6 ± 0.7	2040 ± 90





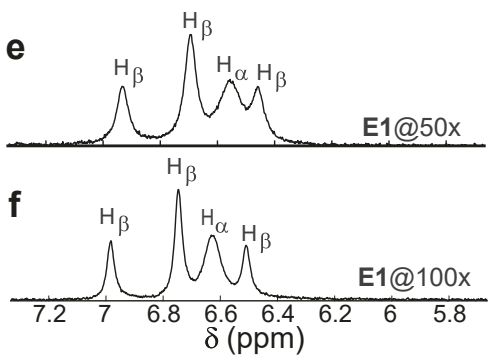


Fig. 3. Experimental 1 H NMR spectra of isoflurane in an **E1** emulsion. **a**) Structure of isoflurane, which contains two unique 1 H nuclei, H_α and H_β , that are assigned in all spectra. 1 H NMR spectra of isoflurane in **b**) pure saline, **c**) pure FC43 solvent (45% isolfurane), **d**) in an undiluted **E1** emulsion and for **e**) 50× and **f**) 100× dilutions of the emulsion. By modeling the chemical shift and line broadening as a function of [Emul] using the Bloch-McConnell equations (McConnell, 1958), both $\kappa_{\rm in}^{\rm NMR}$ and $k_{\rm out}^{\rm NMR}$ and $\epsilon_{\rm out}^{\rm$

nuclei, the 1 H NMR spectra consists of a quartet for the H_α spin and either a doublet of doublets (found in [Fig. 3c] FC43 and in the [Figs. 3d–f] emulsions) or a triplet [Fig. 3b in saline] for the H_β spin. The differences between the isoflurane spectra in saline and FC43 [Fig. 3b vs. Fig. 3c] are due to differences in the chemical environment that isoflurane experiences within the emulsion droplets and in the aqueous phase.

In an emulsion, isoflurane continuously exchanges between emulsion droplets and the aqueous phase:

$$Iso + Emul \underset{\substack{k_{out}^{NMR} \\ something}}{\overset{K_{out}^{NMR}}{\rightleftharpoons}} Iso_{Emul}$$
 (12)

Since the NMR spectra are acquired under equilibrium conditions, the forward and reverse rates in Eq. (12) are equal, i.e.,

$$\kappa_{\text{in}}^{\text{NMR}}[\text{Iso}]_{\text{eq}}[\text{Emul}] = k_{\text{out}}^{\text{NMR}}[\text{Iso}_{\text{Emul}}]_{\text{eq}}$$
(13)

where $[Iso]_{eq}$ and $[Iso_{Emul}]_{eq}$ represent the *sample* equilibrium isoflurane concentrations in the aqueous phase and in the emulsion droplets, respectively, which are given by:

$$\begin{aligned} [\mathrm{Iso}]_{\mathrm{eq}} &= \frac{n_{\mathrm{Iso,eq}}}{V_{\mathrm{tot}}} = \frac{k_{\mathrm{out}}^{\mathrm{NMR}}}{k_{\mathrm{out}}^{\mathrm{NMR}} + k_{\mathrm{in}}^{\mathrm{NMR}}[\mathrm{Emul}]} [\mathrm{Iso}]_{\mathrm{tot}} = \frac{k_{\mathrm{out}}^{\mathrm{NMR}}}{k_{\mathrm{exch}}^{\mathrm{NMR}}} [\mathrm{Iso}]_{\mathrm{tot}} \\ &= \mathrm{Prob}_{\mathrm{ao,eo}}^{\mathrm{Iso}} ([\mathrm{Emul}]) [\mathrm{Iso}]_{\mathrm{tot}} \end{aligned} \tag{14}$$

$$[\mathrm{Iso}_{\mathrm{Emul}}]_{\mathrm{eq}} = \frac{n_{\mathrm{Iso}_{\mathrm{Emul},\mathrm{eq}}}}{V_{\mathrm{tot}}} = \frac{\kappa_{\mathrm{in}}^{\mathrm{NMR}}[\mathrm{Emul}]}{k_{\mathrm{exch}}^{\mathrm{NMR}}}[\mathrm{Iso}]_{\mathrm{tot}} = \mathrm{Prob}_{\mathrm{Emul},\mathrm{eq}}^{\mathrm{Iso}}([\mathrm{Emul}])[\mathrm{Iso}]_{\mathrm{tot}} \quad (15)$$

where $\operatorname{Prob}_{\operatorname{Emul},\operatorname{eq}}^{\operatorname{Iso}}([\operatorname{Emul}])$ and $\operatorname{Prob}_{\operatorname{aq,eq}}^{\operatorname{Iso}}([\operatorname{Emul}])$ are the probabilities of isoflurane to be in either an emulsion droplet or in the aqueous phase, respectively, and $k_{\operatorname{exch}}^{\operatorname{NMR}} = k_{\operatorname{out}}^{\operatorname{NMR}} + \kappa_{\operatorname{in}}^{\operatorname{NMR}}[\operatorname{Emul}]$ is the exchange rate constant with the corresponding isoflurane release time measured by NMR given by:

$$\tau_{\rm NMR} = \frac{1}{k^{\rm NMR}} \tag{16}$$

Although the emulsion samples were always at equilibrium, the exchange process in Eq. (12) still affects the observed NMR spectra depending upon the relative magnitude of $k_{\rm exch}^{\rm NMR}$ and the difference in isoflurane resonance frequencies between the aqueous and organic phases, $|\Delta \nu_{\rm iso}^{\alpha}|=$

$$\left|\frac{\underline{\underline{\gamma}|\overrightarrow{B}|}}{2\pi}\left(\delta_{aq}^{lso,\alpha}-\delta_{FC43}^{lso,\alpha}\right)\right| \text{ and } \left|\Delta\nu_{lso}^{\beta}\right| = \left|\frac{\underline{\underline{\gamma}|\overrightarrow{B}|}}{2\pi}\left(\delta_{aq}^{lso,\beta}-\delta_{FC43}^{lso,\beta}\right)\right|, \text{ where } \delta_{aq}^{lso,\alpha/\beta} \text{ and }$$

 $\delta_{\rm Fmul}^{{
m Iso},\alpha/\beta}$ are the chemical shifts (in ppm) of the α/β resonances in the aqueous

and organic phases, respectively, and $|\overrightarrow{B}|$ is the magnitude of the applied magnetic field. If $k_{\rm exch}^{\rm NMR} \ll 2\pi \left| \Delta \nu_{\rm Iso}^{\alpha/\beta} \right|$, the dynamics, as measured by NMR, are in the slow exchange regime, in which case the NMR spectrum would typically consist of a set of isoflurane resonances in both the aqueous phase [with relative weight of ${\rm Prob}_{\rm ap,eq}^{\rm Iso}([{\rm Emul}])$] and in the emulsion droplets [with relative weight of ${\rm Prob}_{\rm Emul,eq}^{\rm Iso}([{\rm Emul}])$] unless either ${\rm Prob}_{\rm Emul,eq}^{\rm Iso}([{\rm Emul}]) \approx 1$ or ${\rm Prob}_{\rm Emul,eq}^{\rm Iso}([{\rm Emul}]) \approx 0$, in which case only one set of resonances would be observed. If on the other hand $k_{\rm exch}^{\rm NMR} \gg 2\pi \left| \Delta \nu_{\rm Iso}^{\alpha/\beta} \right|$, the dynamics are in the fast-exchange regime, in which case the NMR spectrum would consist of only a single set of isoflurane resonances resonating at the observed frequencies:

$$\nu_{\text{obs}}^{\text{Iso},\alpha/\beta} \approx \text{Prob}_{\text{aq,eq}}^{\text{Iso}}([\text{Emul}])\nu_{\text{aq}}^{\text{Iso},\alpha/\beta} + \text{Prob}_{\text{Emul,eq}}^{\text{Iso}}([\text{Emul}])\nu_{\text{Emul}}^{\text{Iso},\alpha/\beta}$$
(17)

where $\nu_{\text{obs},\alpha/\beta}^{\text{Iso}}$ is simply the weighted average of the isoflurane resonance frequency in the aqueous phase and in the emulsion droplets.

The 1H spectrum of the undiluted **E1** emulsion is shown in Fig. 3d where only a single set of isoflurane resonances was observed. This suggests that the exchange of isoflurane was either in the fast-exchange regime or in the slow-exchange regime but with $\text{Prob}_{\text{Emul},eq}^{\text{Iso}}([\text{Emul}])\approx 1$. To distinguish between these two possibilities, dilution experiments were performed in order to reduce the forward rate in Eq. (13) by reducing [Emul]. The observed frequency shifts of the isoflurane resonances in Figs. 3e and f with increasing dilution were not consistent with $\text{Prob}_{\text{Emul},eq}^{\text{Iso}}([\text{Emul}])\approx 1$, and hence the dynamics could not be in the slow-exchange regime but were instead in the fast-exchange regime. In fact, for the dilution spectra shown in Figs. 3e–f, the observed resonance frequencies were found to fit to the predicted values in the fast exchange regime in Eq. (17) while the observed line widths, $\Delta\nu_{\frac{1}{2},\text{obs}}^{a/\beta}$, were found to fit to the predicted line widths in the fast-exchange regime:

$$\Delta \nu_{\frac{1}{2},\text{obs}}^{a/\beta} = \frac{1}{\pi} \left(\left\langle \frac{1}{T_{2,\text{intrinsic}}^{a/\beta}} \right\rangle + \frac{1}{T_{2,\text{even}}^{a/\beta}} \right) \tag{18}$$

where

$$\left\langle \frac{1}{T_{2,\text{intrinsic}}^{a/\beta}} \right\rangle = \frac{\text{Prob}_{\text{aq,eq}}^{\text{Iso}}([\text{Emul}])}{T_{2,\text{aq}}^{a/\beta}} + \frac{\text{Prob}_{\text{Emul,eq}}^{\text{Iso}}([\text{Emul}])}{T_{2,\text{Emul}}^{a/\beta}}$$
(19)

represents the weighted average of the transverse relaxation rates in the aqueous phase and in the emulsion droplets while

$$\frac{1}{T_{2,\text{exch}}^{\alpha/\beta}} = \frac{(2\pi\Delta\nu_{\text{Iso}}^{\alpha/\beta})^2 \text{Prob}_{\text{aq,eq}}^{\text{Iso}}([\text{Emul}]) \text{Prob}_{\text{Emul,eq}}^{\text{Iso}}([\text{Emul}])}{k_{\text{exch}}}$$
(20)

represents the contribution due to chemical exchange to the line broadening in the fast-exchange limit. As previously demonstrated (Gong et al., 2021), both $\kappa_{\rm in}^{\rm NMR}$ and $k_{\rm out}^{\rm NMR}$ in Eq. (12) can be determined at each dilution by matching the experimentally observed resonance frequencies and line widths to Eqs. (17) and (18), respectively. Simulations using the Bloch-McConnell equations (McConnell, 1958) with $\kappa_{\rm in}^{\rm NMR}$ and $k_{\rm out}^{\rm NMR}$ were found to match the experimental spectra and were consistent with the dynamics being in the fast-exchange regime. Furthermore, the shifting resonances and line broadening followed by line narrowing with increasing dilution observed in Fig. 3 were similar to the behavior found in NMR ligand binding studies in the fast-exchange regime (Fielding, 2007; Lenkinski and Reuben, 1976; Feeney et al., 1975; Sudmeier et al., 1980).

The self-diffusion coefficients for both isoflurane and FC43, which are given in Table 4, were also consistent with the dynamics being in the fast-exchange regime as only a single diffusion coefficient was observed in the decay curves shown in Figs. 4 for the E1 and E2 emulsions. FC43's self-diffusion coefficient was over two-orders-of-magnitude smaller in the emulsion [Fig. 4c] than in an FC43/Iso mixture, further indicating that FC43 was confined to slow moving droplets. The diffusion of isoflurane was also over an order-of-magnitude smaller in the emulsions [Fig. 4b] than in either saline or in pure FC43 as given in Table 4. This was indicative of isoflurane undergoing fast-exchange between the aqueous phase and slow moving droplets.

3.3. Potential limitations and challenges of NMR dilution experiments in determining drug release kinetics

NMR dilution experiments presented in this work are mainly suited towards studying fast releasing drugs from nanocarriers under the conditions where (I) $k_{\rm exch}$ can change by at least a factor of two with dilution and (II) where there exist dilutions such that the line width is dominated by exchange broadening, i.e., $\Delta \nu_{\frac{1}{2},{\rm obs}} \approx \frac{1}{\pi T_{2,{\rm exch}}}$. From the model used in this work and in Ref. (Gong et al., 2021), it was further assumed

that spectral parameters like the intrinsic transverse relaxation times and spin-spin couplings were not changing with dilution and that the intrinsic chemical shifts in the aqueous and hydrophobic phases were determined by a local composition model (Deng et al., 2003; Gong et al., 2021). Deviations from these assumptions or if there are other broadening mechanisms, such as those due to chemical shift anisotropy (Vallurpalli et al., 2008) or residual dipolar couplings (Igumenova et al., 2007) could lead to errors in the NMR-determined rate constants if not properly taken into account (Gong et al., 2021).

Furthermore, the use of dilution experiments requires that the stability of the emulsion droplets under dilution has to be verified in order that the NMR-determined rate constants can be attributed solely to release dynamics and not due to decomposition of the emulsion droplets. For example, it is empirically found that the NMR release time scales with the emulsion droplet volume, i.e., $au_{\rm NMR}{\propto}d_{\rm Emul}^3$ (see Supporting Information for more details). This suggests that a 20% decrease in $d_{\rm Emul}$ could lead to almost a 50% decrease in τ_{NMR} . The rate constants κ_{in}^{NMR} and especially $k_{\mathrm{out}}^{\mathrm{NMR}}$ were also found to change with dilution (see Supporting Information). The observed dilution-dependence of $k_{\text{out}}^{\text{NMR}}$ was attributed to a crowding effect (Gong et al., 2021) that occurs when the distance between emulsion droplets is smaller than the diffusion length over a time τ_{NMR} , $L_D = \sqrt{6D_{\text{Iso,aq}}\tau_{\text{NMR}}}$. For emulsion droplet separations that are larger than $L_D, k_{\mathrm{out}}^{\mathrm{NMR}}$ would correspond to the true rate constant for drug release from an emulsion droplet whereas for droplet separations less than L_D , $k_{\text{out}}^{\text{NMR}}$ would be less than the true release times (for the emulsions studied in this work, $k_{\mathrm{NMR}}^{\mathrm{out}}$ was about a factor of 2 -2.5 times smaller at low dilutions when compared to higher dilutions). While NMR dilution experiments would likely not be appropriate for more slower exchanging drugs, NMR exchange spectroscopy or EXSY (Jeener et al., 1979) could be still used if the exchange rates were faster than the longitudinal relaxation times, or as described in the introduction, q-NMR (Agrahari et al., 2017) could be used to monitor the slow release of drugs in real time. In any case, the NMR methodology presented in this work can be used in a complimentary fashion in order to validate the kinetic parameters derived from other techniques.

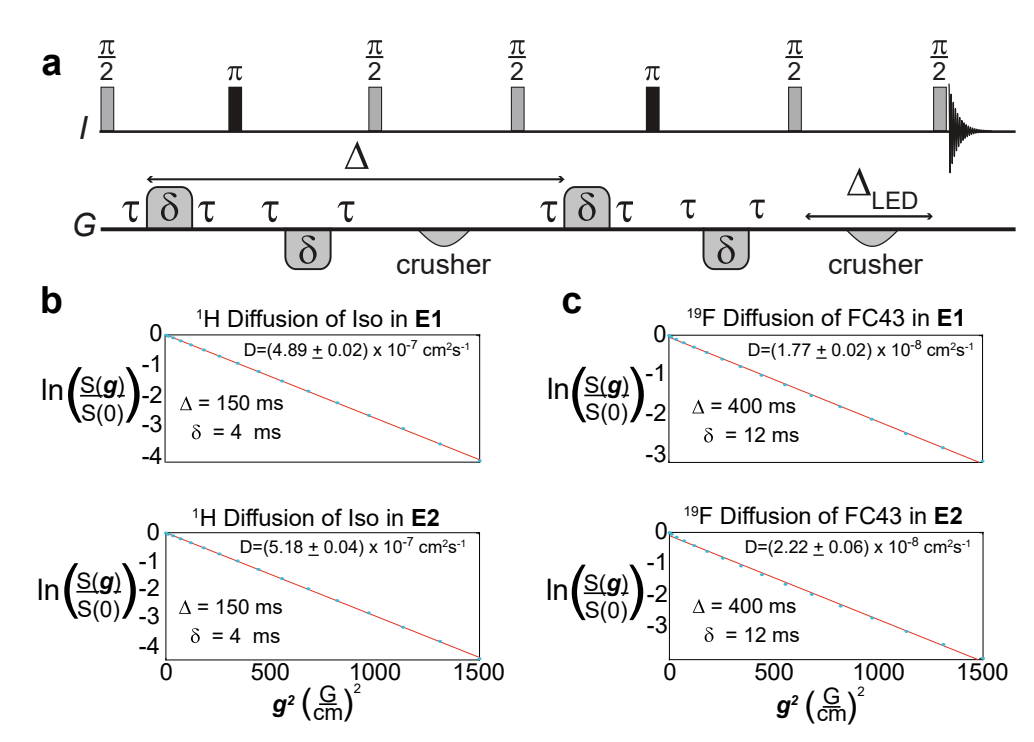


Fig. 4. Diffusion Studies in E1 and E2 emulsion for a series of dilutions. a The selfdiffusion coefficients were measured using the stimulated echo with bipolar gradients and longitudinal eddy delay sequence (Gibbs and Johnson, 1991), where Δ is the diffusion time, δ is the pulsed field gradient length, and Δ_{LED} is the longitudinal eddy current delay. Experimental decay curves, $\ln\left(\frac{S(g)}{S(0)}\right)$ in Eq. (1), acquired on a 400 MHz Bruker spectrometer for (b, 1H NMR) isoflurane and for (c, 19F NMR) FC43 as a function of the square of the pulsed field gradient strength (\mathbf{g}) in the (top) E1 and (bottom) E2 emulsions. Blue dots indicate experimental observations while the red lines represent the best fits to Eq. (1). The following parameters were used in all experiments: $\tau = 200 \, \mu s$, an acquisition time of 1 s, dwell times of 26.5 µs for ¹⁹F and 250 μs for ^{1}H , $\Delta_{LED}=5$ ms, a relaxation delay of $t_d=10$ s, and smooth rectangular shaped pulsed field gradients.

4. Comparison of kinetic parameters derived from reversedialysis and NMR

4.1. In vitro comparisons

The average $k_{\rm out}^{\rm NMR}$ and $\kappa_{\rm in}^{\rm NMR}$ at $100\times$ dilution, which are given in Table 3, were roughly *seven-orders of magnitude* larger than $k_{\rm out}^{\rm R.D.}$ given in Table 2. Furthermore, the reverse-dialysis results in Table 2 suggest that the exchange of isoflurane should be in the slow-exchange regime. To see this, the relationship between $\kappa_{\rm in}^{\rm NMR}$ and $k_{\rm out}^{\rm NMR}$ in Eqs. (12) and (13) with $\kappa_{\rm in}^{\rm R.D.}$ and $k_{\rm out}^{\rm R.D.}$ in Eq. (4) needs to be addressed. The observed signals in NMR are proportional to the amount of isoflurane within the detection volume ($V_{\rm tot}$) whereas in the reverse-dialysis measurements, only the concentration of isoflurane within the aqueous phase is measured.

Comparing τ_{NMR} in Eq. (16) to $\tau_{R.D.}$ in Eq. (9), the effective rate constants derived from reverse-dialysis and NMR are related by:

$$\kappa_{\text{in}}^{\text{NMR}} = \kappa_{\text{in}}^{\text{R.D.}}$$

$$k_{\text{out}}^{\text{NMR}} = k_{\text{out}}^{\text{R.D.}}$$
(21)

For the E1 emulsion, $k_{\rm exch}^{\rm R.D.}=\frac{1}{\tau_{\rm R.D.}}\approx 5\times 10^{-4}{\rm Hz}$ based on the kinetic parameters derived from reverse-dialysis, and since $|\Delta\nu_{\rm Iso}^{\alpha/\beta}|\approx 190-260$ Hz, $k_{\rm exch}\ll 2\pi|\Delta\nu_{\rm Iso}^{\alpha/\beta}$ and so the exchange of isolfurane should be in the slow-exchange regime according to the reverse-dialysis results. From the rate constants determined by reverse-dialysis in Table 2, ${\rm Prob}_{\rm Emul,eq}^{\rm Iso}([{\rm Emul}])=0.43$ and ${\rm Prob}_{\rm aq,eq}^{\rm Iso}([{\rm Emul}])=0.57$, and so isoflurane resonances in both the aqueous phase and in the emulsion droplets should be observed in the NMR spectrum in Figs. ${\bf 3d-f}$, which was not the case. Therefore, the results from reverse-dialysis were inconsistent with the observed NMR spectra of the emulsions. Again, the fact that $\tau_{\rm control}\sim\tau_{\rm R.D.}$ suggests that the reverse-dialysis measurements were not capturing the release of isoflurane from the emulsion droplets but were mainly measuring the transport of isoflurane into a dialysis sac.

4.2. Comparison of reverse-dialysis and NMR-derived rates with respect to in vivo anesthetization of rats: a retrospective analysis

From Table 3, the isoflurane release times derived from NMR were between 106 and 180 μ s for the emulsions studied in this work, whereas the release times from reverse-dialysis were roughly seven orders of magnitude larger, $\tau_{\rm R.D.}\approx 2\times 10^3$ s. Previous in vivo experiments in male Lewis rats (Ashrafi et al., 2018) found an average time for loss of reflexes (ciliary, righting, and pain) of between 69 ± 20 s using an injection rate of the isoflurane emulsion per rat mass of $26.45~\mu L~kg^{-1}~s^{-1}$ (corresponding to an isoflurane content injection rate of 3.81 mg kg $^{-1}s^{-1}$) and a recovery from anesthetization after stopping injection of $\approx\!200~s$. For inhalational dosing of isoflurane, anesthetization in rats was achieved in a time of $38\pm 4~s$, corresponding to a dosing rate per rat mass of $1.5\pm 0.2~mg~kg^{-1}~s^{-1}$. Based on an average rat mass and blood volume of 0.27 kg and 20 mL, respectively, the estimated dilution of the emulsion in the blood was roughly $(29–54)\times$ fold. According to the drug release times

Table 3 NMR-determined rate constants and release times at $100\times$ dilution for the spectrum in Fig. 3f.

Emulsion	$k_{ m out}^{ m NMR} (imes 10^3~{ m s}^{-1})^{ m a}$	$\kappa_{in}^{NMR} \big(\times 10^{11} \; M^{-1} \; s^{-1} \big)^a$	$\tau_{NMR}(\mu s)^b$
E1	5.2 ± 0.5	$\textbf{4.4} \pm \textbf{0.4}$	180 ± 20
E2	8.7 ± 0.6	4.9 ± 0.8	106 ± 8

 $^{^{\}rm a}$ Isoflurane rate constants determined from NMR and averaged over three different replicates at $100\times$ dilution for better comparison to kinetic rate constants derived from reverse-dialysis given in Table 2.

Table 4 Self-diffusion coefficients of isoflurane and FC43 at T=300 K.

$D_{\rm Iso} \left(\times 10^{-7} \; \frac{{ m cm}^2}{{ m s}} \right)^{\rm a}$	$D_{\mathrm{FC43}} \left(\times 10^{-8} \; \frac{\mathrm{cm}^2}{\mathrm{s}} \right)^{\mathrm{b}}$	
E1	4.89 ± 0.02	1.77 ± 0.02
E2	5.18 ± 0.04	2.22 ± 0.06
Iso saturated saline	97 ± 5	-
(1:1 v/v) Iso/FC43	203.4 ± 0.6	890 ± 30

^a Self-diffusion coefficients for isoflurane measured using $^1\mathrm{H}$ diffusion experiments in Fig. 4b.

measured using reverse-dialysis, only 2-3% of isoflurane would have been released from the emulsion droplets within 69 ± 20 s, corresponding to an average dosing rate of $100 \, \mu g \, kg^{-1} \, s^{-1}$. This also corresponds to roughly $\frac{1}{10}$ of the amount of isoflurane necessary to achieve anesthetization by inhalation. As a result, drug release rates measured using reverse-dialysis were inconsistent with previously observed in vivo effects. From the NMR results presented in this work, however, between 72% and 85% of the isoflurane in the emulsion droplets would have been released into the blood, corresponding to an average dosing rate of 3.14 mg $kg^{-1}\ s^{-1}$ over the 69 ± 20 s time period, although based on $k_{\mathrm{exch}}^{\mathrm{NMR}}$, it should be mentioned that the release of isoflurane would have occurred within a time of 0.52-0.85 ms, roughly five orders of magnitude faster than the time for anesthetization to be observed. From these results, the isoflurane release rate does not control the overall pharmacokinetics, and roughly twice more isoflurane needed to be released into the bloodstream from the emulsion to achieve anesthetization than was required from inhalation.

5. Conclusions

In summary, NMR measurements of the isoflurane release times in an emulsified solution of isoflurane in FC43 were found to be seven orders of magnitude faster than those measured using conventional reversedialysis. Furthermore, the NMR derived isoflurane release times were consistent with prior in vivo observations in rats (Ashrafi et al., 2018) whereas those derived from reverse-dialysis were not. The discrepancy between the two measurements is related to fundamental differences between drug release into a dialysis sac as measured by reverse-dialysis versus drug release from sub-micron particles as measured by NMR. NMR is sensitive to differences in the chemical environments between the aqueous and organic phases and is therefore capable of probing the exchange kinetics between phases, even when the exchange is fast. For isoflurane, it appears that the reverse-dialysis measurements in Fig. 2b were only indicative of the rate of diffusion of isoflurane into the dialysis sac, which occurred on a much slower time scale than the actual isoflurane release times from emulsion droplets. Drug release kinetics derived from NMR should prove to be a complementary tool to the development drug/emulsion formulations in the pharmaceutical industry, especially for poorly water-soluble drugs and/or those with fast drug release times.

CRediT authorship contribution statement

Zhaoyuan Gong: Methodology, Software, Validation, Formal analysis, Investigation, Writing – review & editing. Mohammad Hossein Tootoonchi: Conceptualization, Validation, Formal analysis, Investigation, Writing – original draft, Writing – review & editing. Christopher A. Fraker: Conceptualization, Validation, Formal analysis, Investigation, Resources, Supervision, Writing – review & editing, Funding acquisition. Jamie D. Walls: Conceptualization, Methodology, Formal analysis, Resources, Supervision, Writing – original draft, Writing – review & editing, Funding acquisition.

^b Calculated using Eq. (16)

^b Self-diffusion coefficients for FC43 measured using ¹⁹F diffusion experiments in Fig. 4c.

Declaration of Competing Interest

The authors declare that they have no known competing financial interests or personal relationships that could have appeared to influence the work reported in this paper.

Acknowledgement

Research reported in this manuscript was supported by funding from the National Institute of Diabetes and Digestive and Kidney Diseases of the National Institutes of Health under award number R01DK116875, the Diabetes Research Institute Foundation, the National Science Foundation under CHE-1626015 and CHE-1807724, and the University of Miami Center for Computational Science. The content is solely the responsibility of the authors and does not necessarily represent the official views of the National Institutes of Health.

Appendix A. Supplementary material

Brief descriptions of sample preparation and characterization and additional information of the NMR experiments. Supplementary data associated with this article can be found, in the online version, at https://doi.org/10.1016/j.ijpharm.2021.121093.

References

- Abouelmagd, S., Sun, B., Chang, A., Ku, Y., Yeo, Y., 2015. Release kinetics: Study of poorly water-soluble drugs from nanoparticles: Are we doing it right? Mol. Pharm. 12, 997-1003
- Agrahari, V., Meng, J., Purohit, S., Oyler, N., Youan, B.-B., 2017. Real-time analysis of tenofovir release kinetics using quantitative phosphorus (31P) nuclear magnetic resonance spectroscopy. J. Pharm. Sci. 106, 3005–3015.
- Ashrafi, B., Tootoonchi, M., Bardsley, R., Molano, R., Ruiz, P., Jr, E.P., Fraker, C., 2018. Stable perfluorocarbon emulsions for the delivery of halogenated ether anesthetics. Colloids Surf. B: Biointerfaces 172, 797–805.
- Bernkop-Schnurch, A., Jalil, A., 2018. Do drug release studies from SEDDS make any sense? J. Control Release 271, 55–59.
- D'Addio, S., Bukari, A., Dawoud, M., Bunjes, H., Rinaldi, C., Prud'homme, R., 2016.
 Determining drug release rates of hydrophobic compounds from nanocarriers. Phil.
 Trans. R. Soc. A 374, 20150128.
- Deng, D., Li, H., Yao, J., Han, S., 2003. Simple local composition model for ¹H NMR chemical shift of mixtures. Chem. Phys. Lett. 376, 125–129.
- D'Souza, S., DeLuca, P., 2006. Methods to assess in vitro drug release from injectable polymeric particulate systems. Pharm. Res. 23, 460–474.
- Feeney, J., Batchelor, J., Albrand, J., Roberts, G., 1975. The effects of intermediate exchange processes on the estimation of equilibrium constants by NMR. J. Mag. Res. 33, 519–529.
- Fielding, L., 2007. NMR methods for the determination of protein-ligand dissociation constants. Prog. Nucl. Mag. Res. 51, 219–242.
- Forrest, W., Reuter, K., Shah, V., Kazakevich, I., Heslinga, M., Dudhat, S., Patel, S., Neri, C., Mao, Y., 2018. USP Apparatus 4: a valuable in vitro tool to enable formulation development of long-acting parenteral (LAP) nanosuspensions of poorly water-soluble compounds. AAPS PharmSciTech 19, 413–424.
- Fraker, C.A., Mendez, A.J., Inverardi, L., Ricordi, C., Stabler, C.L., 2012. Optimization of perfluoro nanoscale emulsions: The importance of particle size for enhanced oxygen transfer in biomedical applications. Colloids Surf., B 98, 26–35.
- Gibbs, S.J., Johnson, C.S., 1991. A PFG NMR experiment for accurate diffusion and flow studies in the presence of eddy currents. J. Mag. Res. 93, 395–402.
- Gong, Z., Tootoonchi, M.H., Fraker, C.A., Walls, J.D., 2021. Determining chemical exchange rate constants in nanoemulsions using nuclear magnetic resonance. Phys. Chem. Chem. Phys. 23, 19244–19254. https://doi.org/10.1039/D1CP02077C.

- Hey, M.J., Al-Sagheer, F., 1994. Interphase transfer rates in emulsions studied by NMR spectroscopy. Langmuir 10, 1370–1376.
- Igumenova, T.I., Brath, U., Akke, M., Palmer, A.G., 2007. Characterization of chemical exchange using residual dipolar coupling. J. Am. Chem. Soc. 129, 13396–13397.
- Jeener, J., Meier, B.H., Bachmann, P., Ernst, R.R., 1979. Investigation of exchange processes by two-dimensional spectroscopy. J. Chem. Phys 71, 4546–4553.
- Johns, M.L., Hollingsworth, K.G., 2007. Characterisation of emulsion systems using NMR and MRI. Prog. Nucl. Mag. Res. Spect. 50, 51–70.
- Kreilgaard, M., Pedersen, J.J.E.J., 2000. NMR characterisation and transdermal drug delivery potential of microemulsion systems. J. Control Release 69, 421–433.
- Lawson, C.L., Hanson, R.J., 1974. Solving least squares problems. Prentice-Hall Series in Automatic Computation, Englewood Cliffs, N.J.
- Lenkinski, R., Reuben, J., 1976. Line broadenings induced by lanthanide shift reagents: concentration, frequency, and temperature effects. J. Mag. Res. 21, 47–56.
- Levy, M., Benita, S., 1990. Drug release from submicronized o/w emulsion: A new in vitro kinetic evaluation model. Int. J. Pharm. 66, 29–37.
- McConnell, H.M., 1958. Reaction rates by nuclear magnetic resonance. J. Chem. Phys. 28, 430–431.
- Modi, S., Anderson, B.D., 2013. Determination of drug release kinetics from nanoparticles: Overcoming pitfalls of the dynamic dialysis method. Mol. Pharm. 10, 3076–3089.
- Momot, K.I., Kuchel, P.W., 2003. Pulsed field gradient nuclear magnetic resonance as a tool for studying drug delivery systems. Concepts Mag. Res. A 19A, 51–64.
- Momot, K.I., Kuchel, P.W., Chapman, B.E., Deo, P., Whittaker, D., 2003. NMR study of the association of propofol with nonionic surfactants. Langmuir 19, 2088–2095.
- Moreno-Bautista, G., Tam, K., 2011. Evaluation of dialysis membrane process for quantifying the in vitro drug-release from colloidal drug carriers, Colloids and Surfaces A: Physiochem. Eng. Aspects 389, 299–303.
- Omran, A., Kitamura, K., Takegami, S., Kume, M., Yoshida, M., Sayed, A.-A.Y., Mohamed, M., Abdel-Mottaleb, M., 2002. 19F NMR spectrometric determination of the partition coefficients of some fluorinated psychotropic drugs between phosphatidylcholine bilayer vesicles and water, Pharmaceutical and Biomedical. Analysis 30, 1087–1092.
- Petersen, S., Fahr, A., Bunjes, H., 2010. Flow cytometry as a new approach to investigate drug transfer between lipid particles. Mol. Pharm. 7, 350–363.
- Pretto, J., Ricordi, C., Fukawzawa, K., Pileggi, A., Fraker, C., 2016. Stable liquid formulations of volatile gas anesthetics. US Patent 9,308,269.
- Pretto, J., Ricordi, C., Fukawzawa, K., Pileggi, A., Fraker, C., 2018. Stable liquid formulations of volatile gas anesthetics. US Patent 9,980,923.
- Salmela, L., Washington, C., 2014. A continuous flow method for estimation of drug release rates from emulsion formulations. Int. J. Pharm. 472, 276–281.
- Salva, R., Browne, J., Plassat, V., Wasan, K., Wasan, E., 2017. Review and analysis of FDA approved drugs using lipid-based formulations. Drug Dev. Ind. Pharm. 43, 1743–1758.
- Shen, J., Burgess, D., 2013. In vitro dissolution testing strategies for nanoparticulate drug delivery systems: Recent developments and challenges. Drug. Deliv. Trans. Res. 3, 409–415.
- Sinnaeve, D., 2012. The Stejskal-Tanner equation generalized for any gradient shape- an overview of most pulse sequences measuring free diffusion. Conc. Mag. Res. A 40A, 39–65.
- Solomon, D., Gupta, N., Mulla, N., Shukla, S., Guerrero, Y., Gupta, V., 2017. Role of in vitro release methods in liposomal formulation development: Challenges and regulatory perspective. AAPS J. 19, 1669–1681.
- Sudmeier, J.L., Evelhoch, J.L., Johnsson, N.B.-H., 1980. Dependence of NMR lineshape analysis upon chemical rates and mechanisms: Implications for enzyme histidine titrations. J. Mag. Res. 40, 377–390.
- Vallurpalli, P., Hansen, D.F., Kay, L.E., 2008. Probing structure in invisible protein states with anisotropic NMR chemical shifts. J. Am. Chem. Soc. 130, 2734–2735.
- Washington, C., 1989. Evaluation of non-sink dialysis methods for the measurement of drug release from colloids: Effects of drug partition. Int. J. Pharm. 56, 71–74.
- Washington, C., 1990. Drug release from microdisperse systems: A critical review. Int. J. Pharm. 58, 1–12.
- Xie, L., Beyer, S., Vogel, V., Wacker, M., Mantele, W., 2015. Assessing the drug release from nanoparticles: Overcoming the shortcomings of dialysis by using novel optical techniques and a mathematical model. Int. J. Pharm. 488, 108–119.
- Zambito, Y., Pedreschi, E., Colo, G.D., 2012. Is dialysis a reliable method for studying drug release from nanoparticulate systems? A case study. Int. J. Pharm. 434, 28–34.
- Zhong, H., Chan, G., Hu, Y., Ouyang, D., 2018. A comprehensive map of FDA-approved pharmaceutical products. Pharmaceutics 10, 263.